Carrier Phase Navigation Architecture for Shipboard Relative GPS

MOON-BEOM HEO
BORIS PERVAN
Illinois Institute of Technology

Carrier phase differential GPS (DGPS) navigation architectures and algorithms for automatic shipboard landing of aircraft are described. Processing methodologies are defined to provide high integrity carrier phase cycle estimation and positioning by optimally exploiting the complementary benefits of measurement filtering and satellite geometric redundancy for the terminal navigation problem. Navigation performance sensitivity to the standard deviations of raw carrier and code phase measurement errors, measurement error correlation times, and the filtering duration is quantified. Necessary conditions to ensure acceptable terminal navigation availability are specifically defined.

Manuscript received April 12, 2005; revised October 20, 2005; released for publication December 1, 2005.

IEEE Log No. T-AES/42/2/876443.

Refereeing of this contribution was handled by G. Lachapelle.

This work was supported by the United States Navy, Naval Air Warfare Center, N00421-05-C-0008.

The views expressed in this paper are the authors and do not necessarily represent the position of the United States Navy.

Authors' address: Dept. of Mechanical, Material, Aerospace Engineering, Illinois Institute of Technology, Engineering I Bldg., 10 West 32nd St., Chicago, IL 60616-3793, E-mail: (pervan@iit.edu).

I. INTRODUCTION

The joint precision approach and landing system (JPALS) is a differential Global Positioning System (DGPS) architecture that is being developed to provide high accuracy and high integrity navigation for precision approach and landing of military aircraft. An important element of JPALS is shipboard-relative GPS (SRGPS), which is specifically intended to support automatic shipboard landings. Unlike similar operations at ground-based airports, shipboard landing calls for higher navigation performance because of the mobility of the landing platform. The required vertical alert limit (VAL) for the navigation system is 1.1 m, with an associated integrity risk of approximately 10^{-7} [1]. It is desired that these integrity requirements be satisfied with a system availability of at least 99.7% [2]. Because of the stringent nature of these specifications, high-precision carrier phase DGPS solutions are being pursued.

Centimeter-level navigation performance is possible with carrier phase DGPS because carrier ranging measurement errors are normally very small (typically subcentimeter), but the realization of this performance is dependent on the successful resolution of cycle ambiguities. In general, cycle resolution integrity will be a function of the quality of raw code (GPS pseudo-range) and carrier phase measurements, satellite geometry, and filter duration. It is well understood that cycle resolution performance will be best if long filter durations and high performance antennas and receivers (providing small raw code and carrier measurement error) are used.

Initial performance evaluations of SRGPS navigation in [3] assumed that the filtering of ranging measurements was initiated upon aircraft entry into the SRGPS service volume, i.e., within the broadcast range of the shipboard data link. However, it was also noted in [3] that it is possible to begin measurement filtering much earlier. The results of important prior work on filtering in dual-frequency systems [4–6] show that such prefiltering can be especially effective because arbitrarily large filter time constants can be used. One significant implication for the shipboard-relative navigation application is that system requirements on receiver ranging error and/or data broadcast radius can be significantly relaxed. Another is that an SRGPS solution that does not rely on a large data broadcast radius will be implicitly more robust to spatial decorrelation (e.g., tropospheric and ionospheric) error model assumptions.

This research is focused on the design of algorithms for shipboard-relative terminal navigation. A processing methodology is defined to optimally combine the complementary benefits of code and carrier range filtering and satellite geometric redundancy. Specifically, it is proposed that when the aircraft is far from the ship (whether inside or outside the differential service volume), geometry-free filtering is used to estimate GPS L1 minus L2 beat frequency carrier cycle ambiguities—known as the widelane integer ambiguities. In contrast, the use of satellite geometric redundancy for cycle resolution is restricted to the service volume (where the aircraft has access to shipboard reference measurements). Ionospheric and tropospheric propagation errors will be negligibly small when the displacement between the aircraft and ship is small. Thus, when the aircraft is near the ship geometric redundancy is safely exploited for cycle estimation of any remaining widelane integers and, if needed to achieve higher positioning accuracy, individual L1 and L2 integers. By processing this way, performance is greatly enhanced due to the long duration of code measurement filtering, and cycle resolution is robust to spatial decorrelation error model assumptions (because geometric redundancy is used only when the baseline distance is short).

The navigation architecture is described in this work and its fault-free integrity performance is theoretically evaluated relative to the navigation requirements for shipboard landing of aircraft.

II. FUNDAMENTALS OF GEOMETRY-FREE FILTERING

In prefiltering processing at the aircraft, geometry-free code-carrier filtering is executed prior to service volume entry and within the service volume until the aircraft is close to the ship. At the shipboard reference station, the same filter operates continuously. The definitions of the GPS measurements used, the derivation of the filtering algorithm, and a basic performance evaluation are described in this section.

The raw carrier phase GPS measurement is the sum of the true range to the satellite, the cycle ambiguity, and a number of error sources: the satellite and receiver clock biases, spatial decorrelation errors, multipath, and measurement noise. The difference in the raw measurements between the ship and aircraft for a given single satellite is known as a single difference, and it is free of the satellite clock bias. In turn, the receiver clock bias can be eliminated by differencing single difference measurements between two satellites. This is commonly known as a double difference measurement. The double difference carrier phase measurement is the sum of the double difference range, the double difference cycle ambiguity, the double difference spatial decorrelation errors, and the double difference measurement noise and multipath.

An additional difference between L1 and L2 carrier measurements produces a new effective signal with longer wavelength, commonly known as the widelane observable. The details of this measurement form and its usefulness are discussed later in Section IV.

At a given time index k at the aircraft or ship, the raw L1 carrier measurement differenced between two satellites i and j is

$$\lambda_{\mathrm{L1}}\Delta\phi_{\mathrm{L1}}^{ij}(k) = \Delta\rho^{ij}(k) - \Delta I^{ij}(k) + \lambda_{\mathrm{L1}}\Delta N_{\mathrm{L1}}^{ij} + \varepsilon_{\Delta\phi,\mathrm{L1}}^{ij}(k) \tag{1}$$

where $\Delta\rho^{ij}$ is the difference between the sums of the true ranges, tropospheric delays, and satellite clock biases for satellites i and j; λ_{L1} is the wavelength of the L1 signal; ΔI^{ij} is the differential ionospheric propagation delay between the satellites at L1, $\Delta N_{\mathrm{L1}}^{ij}$ is the differential cycle ambiguity, and $\varepsilon_{\Delta\phi,\mathrm{L1}}^{ij}$ is the differential measurement multipath and noise, which is assumed to be normally distributed with zero-mean and standard deviation $\sigma_{\Delta\phi,\mathrm{L1}}^{ij}$. The differenced code phase (pseudo-range) measurement between satellites is similar to (1) except the cycle ambiguity term is absent, the sign on the ionospheric term is opposite, and the standard deviation of the measurement noise is $\sigma_{\Delta PR,\mathrm{L1}}^{ij}$. Nominally, L2 measurements will be available in SRGPS as well. The mathematical expressions for these additional measurements follow:

$$\Delta PR_{\mathrm{L1}}^{ij}(k) = \Delta\rho^{ij}(k) + \Delta I^{ij}(k) + \varepsilon_{\Delta PR,\mathrm{L1}}^{ij}(k) \tag{2}$$

$$\lambda_{\mathrm{L2}}\Delta\phi_{\mathrm{L2}}^{ij}(k) = \Delta\rho^{ij}(k) - \beta\Delta I^{ij}(k) + \lambda_{\mathrm{L2}}N_{\mathrm{L2}}^{ij} + \varepsilon_{\Delta\phi,\mathrm{L2}}^{ij}(k) \tag{3}$$

$$\Delta PR_{\mathrm{L2}}^{ij}(k) = \Delta\rho^{ij}(k) + \beta\Delta I^{ij}(k) + \varepsilon_{\Delta PR,\mathrm{L2}}^{ij}(k) \tag{4}$$

where $\beta = f_{\mathrm{L1}}^2/f_{\mathrm{L2}}^2$ and f_{L1} and f_{L2} are the frequencies of the L1 and L2 carriers, respectively. Equations (1)–(4) can be stacked as follows

$$\begin{bmatrix}\lambda_{\mathrm{L1}}\Delta\phi_{\mathrm{L1}}^{ij}\\ \lambda_{\mathrm{L2}}\Delta\phi_{\mathrm{L2}}^{ij}\\ \Delta PR_{\mathrm{L1}}^{ij}\\ \Delta PR_{\mathrm{L2}}^{ij}\end{bmatrix} = \begin{bmatrix}1 & -1\\ 1 & -\beta\\ 1 & 1\\ 1 & \beta\end{bmatrix}\begin{bmatrix}\Delta\rho^{ij}\\ \Delta I^{ij}\end{bmatrix} + \begin{bmatrix}\lambda_{\mathrm{L1}} & 0\\ 0 & \lambda_{\mathrm{L2}}\\ 0 & 0\\ 0 & 0\end{bmatrix}\begin{bmatrix}\Delta N_{\mathrm{L1}}^{ij}\\ \Delta N_{\mathrm{L2}}^{ij}\end{bmatrix} + \begin{bmatrix}\Delta\varepsilon_{\Delta\phi,\mathrm{L1}}^{ij}\\ \Delta\varepsilon_{\Delta\phi,\mathrm{L1}}^{ij}\\ \Delta\varepsilon_{\Delta PR,\mathrm{L2}}^{ij}\\ \Delta\varepsilon_{\Delta PR,\mathrm{L2}}^{ij}\end{bmatrix}. \tag{5}$$

For simplicity of notation, (5) is rewritten as

$$z = A\begin{bmatrix}\Delta\rho^{ij}\\ \Delta I^{ij}\end{bmatrix} + B\begin{bmatrix}\Delta N_{\mathrm{L1}}^{ij}\\ \Delta N_{\mathrm{L2}}^{ij}\end{bmatrix} + \nu. \tag{6}$$

Since we are only interested in extracting information on the cycle ambiguities in the prefiltering phase, (6) can be further simplified by premultiplying both sides of the equation by a matrix L, which forms an orthonormal basis for the left null space of the matrix A:

$$Lz = LB\begin{bmatrix}\Delta N_{\mathrm{L1}}^{ij}\\ \Delta N_{\mathrm{L2}}^{ij}\end{bmatrix} + L\nu. \tag{7}$$

The error in the estimate of differential cycle ambiguities obtained from solving (7) is described by the covariance matrix

$$P_{\Delta N} = (H_f^T R_e^{-1} H_f)^{-1} \tag{8}$$

where $H_f = LB$ and $R_e = LV_v L^T$. V_v is the 4×4 diagonal matrix

$$V_v = \begin{bmatrix} (\sigma^{ij}_{\Delta\phi,\mathrm{L1}})^2 & 0 & 0 & 0 \\ 0 & (\sigma^{ij}_{\Delta\phi,\mathrm{L2}})^2 & 0 & 0 \\ 0 & 0 & (\sigma^{ij}_{\Delta PR,\mathrm{L1}})^2 & 0 \\ 0 & 0 & 0 & (\sigma^{ij}_{\Delta PR,\mathrm{L2}})^2 \end{bmatrix}. \tag{9}$$

In this work, we assume that $\sigma^{ij}_{\Delta\phi,\mathrm{L1}} = \sigma^{ij}_{\Delta\phi,\mathrm{L2}} \equiv \sigma_{\Delta\phi}$ and $\sigma^{ij}_{\Delta PR,\mathrm{L1}} = \sigma^{ij}_{\Delta PR,\mathrm{L2}} \equiv \sigma_{\Delta PR}$. An eigenvector decomposition of the covariance matrix $P_{\Delta N} = VDV^T$ is quantified below assuming $\sigma_{\Delta\phi} = 1$ cm and $\sigma_{\Delta PR} = 30$ cm:

$$D = \begin{bmatrix} 0.03113 & 0 \\ 0 & 129.71 \end{bmatrix} \qquad V = \begin{bmatrix} 0.70444 & -0.70977 \\ -0.70977 & -0.70444 \end{bmatrix} \tag{10}$$

where D and V are, respectively, the eigenvalue and eigenvector matrices for $P_{\Delta N}$. This analysis result, initially revealed by Euler and Goad [4] using a Kalman filter approach, shows that observability of the individual cycle ambiguities, $\Delta N^{ij}_{\mathrm{L1}}$ and $\Delta N^{ij}_{\mathrm{L2}}$, using (7) is poor, but that relatively strong information on the widelane ambiguity $\Delta N^{ij}_{\mathrm{L1}} - \Delta N^{ij}_{\mathrm{L2}}$ is gained. Widelane ambiguity observability can be further greatly enhanced by filtering observable (7) over time. The details of a more practical filtering implementation are described in Appendices A and B. Therefore, it is interesting to consider whether a navigation architecture based on knowledge of widelane integers (rather than the individual L1 and L2 cycle ambiguities) is sufficient to meet SRGPS requirements. This question is answered in the analysis that follows.

III. SIMPLE ANALYSIS BASED ON VDOP

Fig. 1 shows the availability of vertical dilution of precision (VDOP) using only satellites that have been in view for specified prefiltering durations. The use of VDOP in this preliminary analysis implicitly assumes that all satellite ranging errors have equal variances. However, the results are nevertheless useful (if somewhat conservative) if the variance for the worst case satellite (typically lowest elevation) is considered. In Fig. 1, the vertical axis defines the fraction of time that the VDOP is equal to or smaller than the values defined on the horizontal axis. To generate the results in this plot, the nominal DO229A (WAAS MOPS) GPS satellite constellation, a representative central Pacific location (22 deg N, 158 deg W) with 1 min sampling interval, and 7.5 deg elevation mask angle were used. The effect of depleted GPS satellite constellations were also included in these results—and all subsequent availability results in this paper—using the minimum standard constellation state probability model provided in the GPS Standard Positioning Service Performance Standard [7]. The state probability model used is given in Table I, and the methodology used to perform the availability assessments follows the work of Shively in [11]. The values in parenthesis next to each curve in Fig. 1, are the maximum VDOPs that must be managed in order to meet the SRGPS availability requirement of 99.7% using only satellites that have been available for the entire specified prefiltering time. In reality, satellites that have been in view for shorter duration are also potentially useful, but they are neglected in this first (conservative) analysis. These satellites are accounted for in the detailed analyses in the following sections of this paper, as are other user locations.

TABLE I
GPS Constellation Availability

Number of Healthy Satellites	State Probability
24	0.95
23	0.03
22	0.012
21	0.005
20	0.003

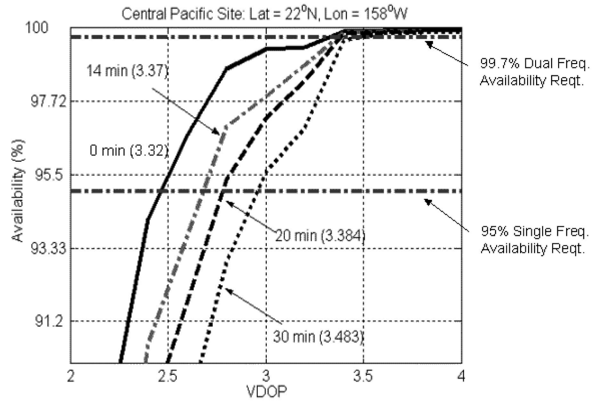

Fig. 1. Availability versus VDOP.

Given the required VDOP to meet the SRGPS availability specification, and assuming for the moment that the widelane integers are known and fixed, it is possible to compute the maximum permissible standard deviation for the widelane single difference carrier phase:

$$\mathrm{VPL} = \sigma_{\Delta\phi,w} \cdot \mathrm{VDOP} \cdot K_{ffd} < 1.1 \text{ m} \tag{11}$$

where VPL is the vertical protection level, $\sigma_{\Delta\phi,w}$ is the standard deviation for the widelane single difference carrier phase, and $K_{ffd} = 5.33$ is the integrity multiplier corresponding to the integrity risk requirement of 10^{-7}. ($K_{ffd} = 2Q^{-1}(10^{-7})$, where Q is the standard normal cumulative distribution function.)

The relevance of inequality (11) is readily seen through a simple example. Using only satellites that have been available for 30 min of prefiltering or longer, the maximum VDOP (to ensure 99.7% availability) is about 3.5. In this case, using (11), it is required that $\sigma_{\Delta\phi,w} < 5.93$ cm. The relationship between the single difference carrier and single difference widelane carrier standard deviation is given in [8]:

$$\sigma_{\Delta\phi,w} = 5.74\sigma_{\Delta\phi} \tag{12}$$

where $\sigma_{\Delta\phi}$ is the single difference carrier standard deviation. Therefore, the required value of $\sigma_{\Delta\phi}$ is 1.03 cm or less, which is achievable using modern GPS receivers, but must be experimentally verified for the high-multipath shipboard landing environment.

In this simple analysis to determine the required value of $\sigma_{\Delta\phi}$, it was assumed that the widelane integers were known after 30 min of prefiltering of observable (7). We now turn our attention to determine the required value of the raw code difference standard deviation ($\sigma_{\Delta PR}$) to ensure that the likelihood of incorrect cycle resolution is consistent with SRGPS integrity requirements. Fig. 2 quantifies the sensitivity of floating widelane ambiguity estimate error, σ_w, to $\sigma_{\Delta PR}$, given that $\sigma_{\Delta\phi} = 1$ cm. In this analysis, it was assumed that $\sigma_{\Delta\phi}$ of 1 cm is same for any satellite elevation angle, and overbounds the standard deviation of the single difference carrier phase measurement error at 7.5° satellite elevation angle. The dashed-dot horizontal line in the figure is the maximum value of σ_w required to ensure a 10^{-8} total probability of incorrect integer rounding for eight satellites. In these results, ranging error for both code and carrier was modeled as a first-order Gauss-Markov random process with a time constant of 1 min. (Some details of the implementation of this error model are discussed in Appendix B.) As an example, given a geometry-free filtering duration of 30 min, the widelane integers can be fixed with the specified integrity only if $\sigma_{\Delta PR}$ is 27 cm or smaller.

This requirement for raw code error is very stringent, but may be achievable using state-of-the-art receivers and antennas currently under development for SRGPS. Nevertheless, in the sections that follow we show that this requirement can be relaxed by exploiting geometric redundancy when the aircraft is close to the ship, and processing L1 and L2 measurements directly (rather than widelane only). In addition, we also quantify in detail the sensitivity of performance to $\sigma_{\Delta\phi}$ and $\sigma_{\Delta PR}$, code error time constant, and prefiltering time.

The output of the prefiltering process at both the aircraft and ship is a vector of floating widelane

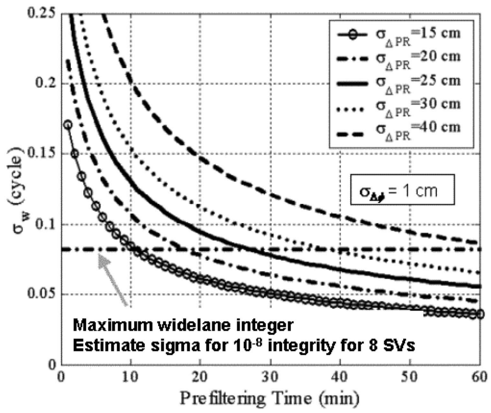

Fig. 2. Widelane cycle resolution.

cycle ambiguity estimates, $[\Delta\hat{N}_w^{12} \cdots \Delta\hat{N}_w^{1n}]^T$, and the associated estimate error covariance matrix, $P_{\Delta N,w}$. Here n is the number of satellites, and a satellite which has been in view for the entire prefiltering duration (arbitrarily chosen to be satellite index 1 here) is selected as the master for differencing. Prefiltering data from the aircraft and ship may be combined when the aircraft is close to the ship to obtain the double difference cycle ambiguity vector $[\nabla\Delta\hat{N}_w^{12} \cdots \nabla\Delta\hat{N}_w^{1n}]^T$ and associated covariance matrix $P_{\nabla\Delta N,w} = P_{\Delta N,w_{\rm air}} + P_{\Delta N,w_{\rm ship}}$.

IV. WIDELANE ARCHITECTURE WITH GEOMETRY-FREE FILTERING

Within the SRGPS service volume, the double difference carrier phase measurements for L1 and L2 and satellites i and j can be written as follows:

$$\lambda_{L1}\nabla\Delta\phi_{L1}^{ij} = -(e^{i^T} - e^{j^T})x - \nabla\Delta I^{ij} + \nabla\Delta T^{ij} + \lambda_{L1}\nabla\Delta N_{L1}^{ij} + \varepsilon_{\nabla\Delta\phi,L1}^{ij} \tag{13}$$

$$\lambda_{L2}\nabla\Delta\phi_{L2}^{ij} = -(e^{i^T} - e^{j^T})x - \beta\nabla\Delta I^{ij} + \nabla\Delta T^{ij} + \lambda_{L2}\nabla\Delta N_{L2}^{ij} + \varepsilon_{\nabla\Delta\phi,L2}^{ij} \tag{14}$$

where e^i is the line of sight vector to the satellite i, x is the aircraft position vector relative to the ship, $\nabla\Delta I^{ij}$ is the double difference ionospheric propagation delay for the satellites at L1, and $\nabla\Delta T^{ij}$ is the double difference tropospheric delay, ε^{ij} terms are the double difference code and carrier measurement errors due to receiver noise and multipath. When the aircraft is close to the ship (at 0.25 nmi distance and 100 ft height) the tropospheric and ionospheric spatial decorrelation errors are negligible.

Omitting the ionospheric and tropospheric terms in the L1 and L2 double difference measurements (13) and (14), the double difference widelane carrier measurement can be constructed as follows:

$$\lambda_w \nabla\Delta\phi_w^{ij} = \lambda_w(\nabla\Delta\phi_{L1}^{ij} - \nabla\Delta\phi_{L2}^{ij})$$
$$= -(e^{i^T} - e^{j^T})x + \lambda_w \nabla\Delta N_w^{ij} + \varepsilon_{\nabla\Delta\phi,w}^{ij} \quad (15)$$

where the widelane wavelength $\lambda_w = c/(f_{L1} - f_{L2})$, c is the speed of light, $\nabla\Delta N_w^{ij}$ is the double difference widelane integer for satellites i and j, and $\varepsilon_{\nabla\Delta\phi,w}^{ij}$ is the double difference widelane carrier measurement error due to receiver noise and multipath. The widelane measurement (15) can also be expressed in vector form as follows:

$$[\nabla\Delta\phi_w] = [G_{(n-1)\times 3} \;\; I_{(n-1)\times(n-1)}] \begin{bmatrix} x_{3\times 1}/\lambda_w \\ \nabla\Delta N_{w,(n-1)\times 1} \end{bmatrix} + \nu \quad (16)$$

where $x_{3\times 1}$ is the 3×1 aircraft position vector relative to the ship, $\nabla\Delta N_{w,(n-1)\times 1}$ is the $(n-1)\times 1$ double difference widelane integer vector, $I_{(n-1)\times(n-1)}$ is the $(n-1)\times(n-1)$ identity matrix, and $G_{(n-1)\times 3}$ is the $(n-1)\times 3$ geometry matrix $[-(e^1 - e^2)\cdots-(e^1 - e^n)]^T$.

It is relatively simple to fuse the output of the prefiltering process into double difference widelane positioning because the output of the former is the floating estimate of the double difference widelane cycle ambiguity vector:

$$\begin{bmatrix} \nabla\Delta\hat{N}_w^{12} \\ \vdots \\ \nabla\Delta\hat{N}_w^{1n} \end{bmatrix} = I_{(n-1)\times(n-1)} \begin{bmatrix} \nabla\Delta N_w^{12} \\ \vdots \\ \nabla\Delta N_w^{1n} \end{bmatrix} + \nu_N. \quad (17)$$

In (17), $\nabla\Delta\hat{N}_w^{1n}$ is the floating double difference widelane cycle ambiguity estimate for satellites 1 and n obtained as a result of prefiltering, $\nabla\Delta N_w^{1n}$ is the true double difference widelane integer, and ν_N is the cycle ambiguity estimate error from prefiltering, which has covariance matrix $P_{\nabla\Delta N,w}$. At this point, depending on the duration of prefiltering for the individual satellites, it may be possible to round widelane ambiguities. In this regard, all possible cycle ambiguities are fixed subject to the constraint that the probability of fixing one or more incorrect integers is lower than 10^{-8} (comfortably below the overall integrity risk requirement of 10^{-7}). For the remaining cycle ambiguities, a floating estimate vector and covariance matrix must be retained. Substituting these results into (16), it is possible to obtain the aircraft position and position error covariance. Finally, the vertical error standard deviation is scaled by K_{ffd} to produce the VPL, which is compared with VAL (1.1 m) determine whether sufficient performance is available for aircraft landing.

Using the processing architecture defined above, SRGPS availability has been evaluated for various values of single difference carrier and code phase measurement error standard deviation for a central

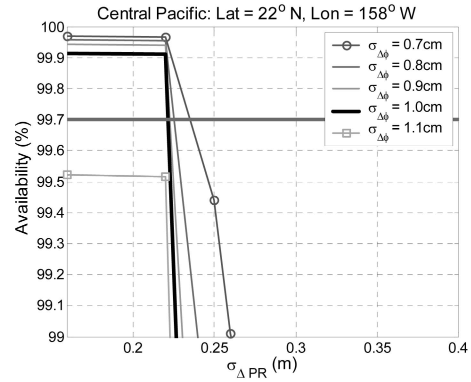

Fig. 3(a). Availability for widelane architecture for $\psi = 20$.

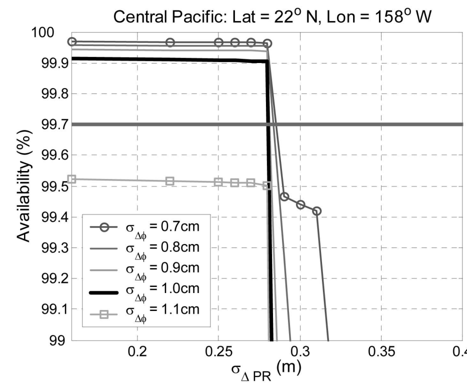

Fig. 3(b). Availability for widelane architecture for $\psi = 30$.

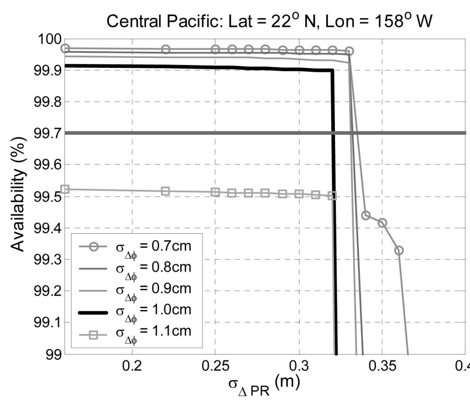

Fig. 3(c). Availability for widelane architecture for $\psi = 40$.

Pacific ship location (22 deg N and 128 deg W). The satellite outage state probability model in Table I and a 7.5 deg elevation mask angle were assumed in this analysis. Figs. 3(a)–3(c) quantify the sensitivity of the availability to the prefiltering duration, which is expressed in terms of the nondimensional ratio

$$\psi = \frac{T}{\tau} \quad (18)$$

where T is the filtering time, and τ is the code measurement error time constant. Results were computed for three different values of the ratio ψ (20, 30, and 40). The performance of the prefiltering process is sensitive to this nondimensional ratio because it is related to the maximum effective number of independent measurement updates available during prefiltering.

These figures can be used to derive the required single difference standard deviation of code ($\sigma_{\Delta PR}$) and carrier ($\sigma_{\Delta\phi}$) phase measurements to ensure 99.7% availability. From the results, it is clear that as ψ increases, the required $\sigma_{\Delta PR}$ also increases. It is also evident that the required $\sigma_{\Delta PR}$ is more sensitive than $\sigma_{\Delta\phi}$ to variations in ψ. For example, as ψ varies from 20 to 40, the required $\sigma_{\Delta PR}$ is relaxed from 22 cm up to 32 cm. In contrast, the required maximum $\sigma_{\Delta\phi}$ remains 1 cm, for values of $\psi = 20$, 30, and 40. This result is consistent with the simpler, conservative analysis in Section II, which showed that when only widelane measurements are used (as is the case here), values of $\sigma_{\Delta\phi}$ larger than about 1 cm will not provide sufficiently accurate positioning to ensure 99.7% availability even if all of the widelane integers are correctly fixed.

V. WIDELANE ARCHITECTURE WITH GEOMETRY-FREE FILTERING AND GEOMETRIC REDUNDANCY

The use of geometric redundancy provides two significant improvements to the simple processing structure described above:

1) increased availability,
2) relaxation of the required $\sigma_{\Delta\phi}$ and $\sigma_{\Delta PR}$.

However, the use of geometric redundancy introduces ionospheric and tropospheric spatial decorrelation error into the cycle resolution process. Any residual effects of these errors can be statistically handled by increasing the standard deviation of the single difference measurements as a function of distance and height, but the robustness of any particular model will always be questionable over extended distances. To ensure cycle resolution integrity for safety-of-life applications such as SRGPS, geometric redundancy should be used only if the displacement between the aircraft and ship is small. (If the displacement is small, then the spatial decorrelation error is small.) For example, given that the 1.1 m VAL is applicable at 100 ft altitude for SRGPS, this corresponds to a displacement of about 0.25 nmi at which geometric redundancy can be exploited.

When geometric redundancy is used, integer fixing is attempted after (16) and (17) are combined. However, the geometric (16) introduces further correlation between the cycle ambiguity states, making it difficult to treat satellites cycle ambiguities individually. To address the issue, we make use of Teunissen's LAMBDA cycle ambiguity decorrelation algorithm with integer bootstrapping [9]. This implementation is a successive rounding approach that has the following two significant benefits for our application.

1) The probability of correct fix can be computed directly.

2) Fixing can be restricted to only those cycle ambiguities (or linear combinations thereof) which have high enough probability of correct fix to meet the integrity requirement.

For this application, it was determined whether for some (or all) independent linear combinations of cycle ambiguities the probability of correct fix is larger than $1 - 10^{-8}$. If so, the position error covariance was updated assuming the associated integers were precisely known. For the remaining cycle ambiguities, the floating estimates (and covariances) were retained.

The resulting availability of this double difference widelane architecture, which uses both geometry-free prefiltering and geometric redundancy, was evaluated for various values of $\sigma_{\Delta\phi}$ and $\sigma_{\Delta PR}$. The sensitivity of availability to nondimensional time ratio ψ is also shown in Figs. 4(a)–4(c). These results were generated for the same ship location and elevation mask used in the last section. When compared with the previous results (which used the double difference widelane without geometric redundancy) for any given value of ψ, the new results show that the required $\sigma_{\Delta PR}$ is relaxed significantly. As an example, given $\sigma_{\Delta\phi} = 1$ cm and $\psi = 30$, the required $\sigma_{\Delta PR}$ is 35 cm or less with geometric redundancy and 28 cm or less without. However, it is also evident in the comparison between the results in Fig. 3 and 4 that the required $\sigma_{\Delta\phi}$ does not deviate from 1 cm. Again, this is due to the fact that a single difference standard deviation of 1 cm is necessary to ensure widelane carrier phase positioning availability even if all widelane cycle ambiguities are correctly fixed. It is natural then to consider the potential benefits of processing L1 and L2 measurements directly (rather than using widelane measurements) when the aircraft is close to the ship. This approach is explored in the next section.

VI. L1/L2 ARCHITECTURE WITH GEOMETRY-FREE FILTERING AND GEOMETRIC REDUNDANCY

The double difference measurements (13) and (14) in cycles can be written as

$$\begin{bmatrix} \nabla\Delta\phi_{L1} \\ \nabla\Delta\phi_{L2} \end{bmatrix} = H \begin{bmatrix} x_{3\times1}/\lambda_{L1} \\ \nabla\Delta N_{L1,(n-1)\times1} \\ \nabla\Delta N_{L2,(n-1)\times1} \end{bmatrix} + \nu_{\nabla\Delta} \qquad (19)$$

where $\nabla\Delta N_{L1,(n-1)\times1}$ is the $(n-1)\times1$ double difference integer for the L1 carrier measurements, $\nabla\Delta N_{L2,(n-1)\times1}$ is the $(n-1)\times1$ double difference integer for the L2 carrier measurements, and $\nu_{\nabla\Delta}$ is the double difference measurement noise in cycles.

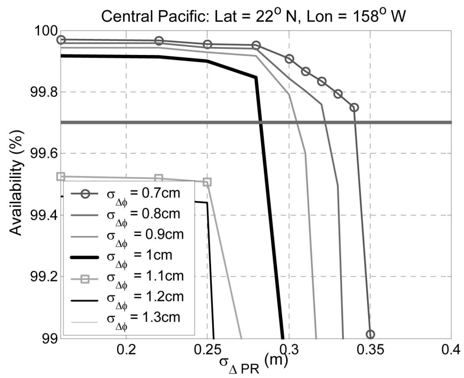

Fig. 4(a). Availability for widelane architecture with geometric redundancy with $\psi = 20$.

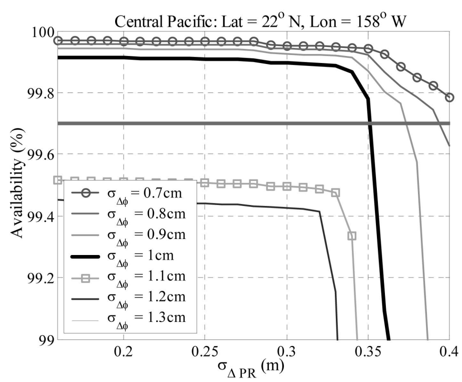

Fig. 4(b). Availability for widelane architecture with geometric redundancy with $\psi = 30$.

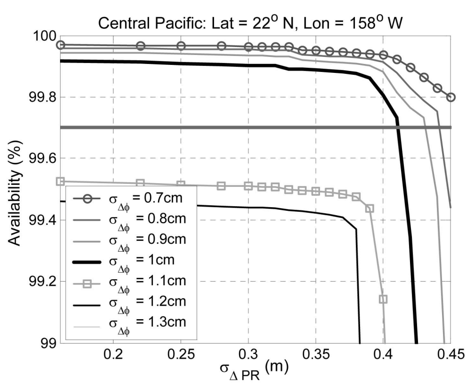

Fig. 4(c). Availability for widelane architecture with geometric redundancy with $\psi = 40$.

The position states in (19) are expressed in L1 cycles. The observation matrix H is

$$H = \begin{bmatrix} G_{(n-1)\times 3} & I_{(n-1)\times(n-1)} & 0_{(n-1)\times(n-1)} \\ G_{(n-1)\times 3} \times \lambda_{L1}/\lambda_{L2} & 0_{(n-1)\times(n-1)} & I_{(n-1)\times(n-1)} \end{bmatrix} \tag{20}$$

where $G_{(n-1)\times 3}$ is the double difference geometry matrix which was defined below (16). To fuse the prefiltering information (the floating double difference widelane cycle ambiguity estimate vector and its associated covariance matrix) into (19), we need to construct the double difference widelane integer observable from the double difference L1/L2 carrier phase integers as in (17). In this case the appropriate mathematical expression is

$$\begin{bmatrix} \nabla\Delta\hat{N}_w^{12} \\ \vdots \\ \nabla\Delta\hat{N}_w^{1n} \end{bmatrix} = J \begin{bmatrix} \nabla\Delta N_{L1}^{12} \\ \vdots \\ \nabla\Delta N_{L1}^{1n} \\ \nabla\Delta N_{L2}^{12} \\ \vdots \\ \nabla\Delta N_{L2}^{1n} \end{bmatrix} + v_N \tag{21}$$

where $\nabla\Delta N_{L1}^{1n}$ is the true double difference L1 integer, $\nabla\Delta N_{L2}^{1n}$ is the true double difference L2 integer, and v_N is the cycle ambiguity estimate error from prefiltering, which has covariance matrix $P_{\nabla\Delta N,w}$. J is the integer coefficient matrix which defines the relationship between the double difference widelane carrier and double difference L1/L2 carrier integers. Its mathematical expression is

$$J = [I_{(n-1)\times(n-1)} \;\; -I_{(n-1)\times(n-1)}]. \tag{22}$$

Given (21), the covariance matrix of double difference L1/L2 carrier phase cycle ambiguities was extracted from $P_{\nabla\Delta N,w}$, the covariance matrix output from the prefiltering process. Then the L1 and L2 cycle ambiguity state covariance was refined using geometric redundancy (19), as described in the previous section for widelane ambiguities. The aircraft position covariance was then computed and compared with the VAL.

The simulation results, using the same ship location, elevation mask, and measurement error parameters as those in Figs. 3 and 4, are shown in Figs. 5(a)–5(c). In comparison with the results on the prior figures, Fig. 5 shows that L1/L2 processing provides further performance improvement. Specifically, it is evident that for any given time ratio ψ, L1/L2 processing enables relaxation of the required values of both $\sigma_{\Delta PR}$ and $\sigma_{\Delta\phi}$. The required $\sigma_{\Delta\phi}$ is especially notable, since it was invariant in the previous results and showed significant performance degradation below 1 cm. While the relaxation in $\sigma_{\Delta\phi}$ is modest here, it is important to observe that performance degrades gracefully as $\sigma_{\Delta\phi}$ increases. In contrast, the performance of both widelane architectures is severely affected when $\sigma_{\Delta\phi}$ is larger than 1 cm.

To observe the sensitivity of availability of L1/L2 processing to ship location, results were also computed for three other ship locations, near China (20 deg N, 120 deg E), in the Atlantic Ocean (25 deg N, −30 deg E), and at an alternate Pacific Ocean location (35 deg N, −158 deg E). These simulation results, which are shown in Figs. 6(a)–6(c), used the time ratio $\psi = 30$ and the same elevation mask and measurement error parameters that were used to generate Figs. 3, 4, and 5. The results show

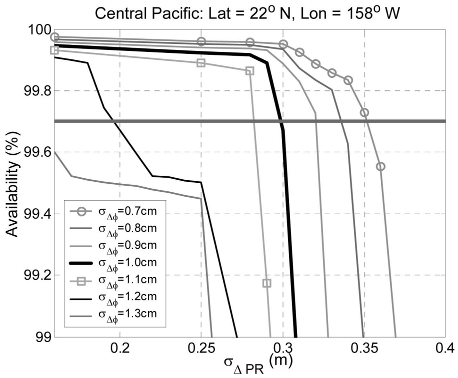

Fig. 5(a). Availability for L1/L2 architecture with geometric redundancy with $\psi = 20$.

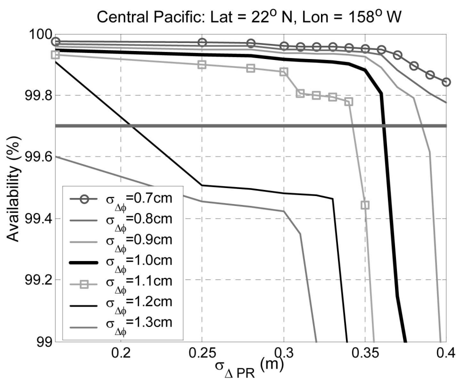

Fig. 5(b). Availability for L1/L2 architecture with geometric redundancy with $\psi = 30$.

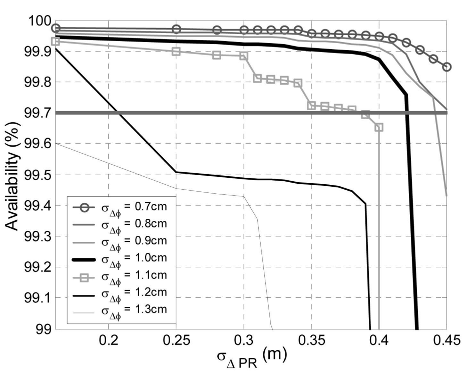

Fig. 5(c). Availability for L1/L2 architecture with geometric redundancy with $\psi = 40$.

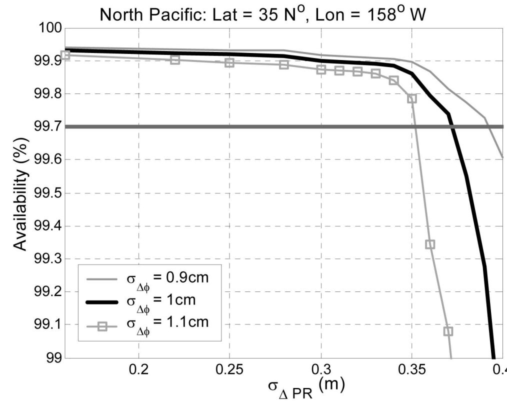

Fig. 6(a). Availability for L1/L2 architecture at another Pacific Ocean location with $\psi = 30$.

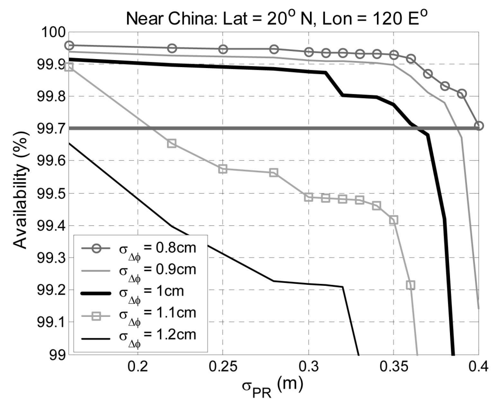

Fig. 6(b). Availability for double difference L1/L2 carrier phase using geometric redundancy near China with $\psi = 30$.

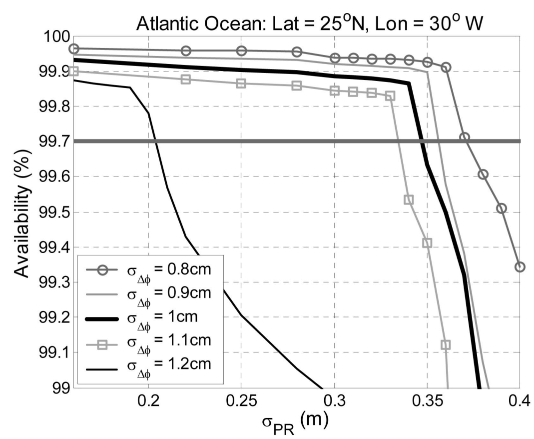

Fig. 6(c). Availability for double difference L1/L2 carrier phase using geometric redundancy at Atlantic Ocean with $\psi = 30$.

that for $\sigma_{\Delta\phi}$ = 1 cm, the required $\sigma_{\Delta PR}$ to ensure 99.7% SRGPS availability exhibits mild sensitivity to the ship location, ranging from 34.5–37 cm. A worldwide geographical sensitivity analysis is the subject of continuing work.

VII. CONCLUSIONS

This paper was focused on the design of robust airborne algorithms for shipboard-relative navigation of aircraft using carrier phase DGPS measurements. Three processing methodologies were defined to provide high integrity carrier phase cycle estimation and positioning for terminal navigation by optimally exploiting the complementary benefits of measurement filtering and satellite geometric redundancy. These algorithms were based on

1) geometry-free prefiltering and near-ship positioning using widelane observables exclusively,

2) geometry-free prefiltering with near-ship geometric redundancy and positioning using widelane observables exclusively,

3) geometry-free widelane prefiltering and L1/L2 near-ship geometric redundancy and positioning.

Detailed covariance analysis results showed that the best performance for shipboard-relative terminal navigation is achieved using the third processing architecture. In addition, the sensitivity of navigation performance to the standard deviations of raw carrier and code phase measurements, measurement error correlation times, and the filtering duration was quantified. Necessary conditions on these parameters to ensure acceptable terminal navigation availability were specifically defined.

APPENDIX A. WIDELANE CYCLE AMBIGUITY ESTIMATION

Given the differenced carrier phase (1) and (3), the differenced widelane carrier phase observable can be written as

$$\Delta\phi_{\mathrm{L1}} - \Delta\phi_{\mathrm{L2}} = \Delta\rho\left(\frac{1}{\lambda_{\mathrm{L1}}} - \frac{1}{\lambda_{\mathrm{L2}}}\right) + \Delta I\left(-\frac{1}{\lambda_{\mathrm{L1}}} + \beta\frac{1}{\lambda_{\mathrm{L2}}}\right) + (\Delta N_{\mathrm{L1}} - \Delta N_{\mathrm{L2}}) + \left(\frac{\varepsilon_{\Delta\phi,\mathrm{L1}}}{\lambda_{\mathrm{L1}}} - \frac{\varepsilon_{\Delta\phi,\mathrm{L2}}}{\lambda_{\mathrm{L2}}}\right). \tag{23}$$

Normalizing the differenced code measurement (2) and (4) by carrier wavelength and adding the results produces the narrowlane code measurement. The mathematical expression is

$$\frac{\Delta PR_{\mathrm{L1}}}{\lambda_{\mathrm{L1}}} + \frac{\Delta PR_{\mathrm{L2}}}{\lambda_{\mathrm{L2}}} = \Delta\rho\left(\frac{1}{\lambda_{\mathrm{L1}}} + \frac{1}{\lambda_{\mathrm{L2}}}\right) + \Delta I\left(\frac{1}{\lambda_{\mathrm{L1}}} + \beta\frac{1}{\lambda_{\mathrm{L2}}}\right) + \left(\frac{\varepsilon_{\Delta PR,\mathrm{L1}}}{\lambda_{\mathrm{L1}}} + \frac{\varepsilon_{\Delta PR,\mathrm{L2}}}{\lambda_{\mathrm{L2}}}\right). \tag{24}$$

Equations (23) and (24) can be rearranged to obtain

$$\Delta\phi_{\mathrm{L1}} - \Delta\phi_{\mathrm{L2}} = \Delta\rho\left(\frac{\lambda_{\mathrm{L2}} - \lambda_{\mathrm{L1}}}{\lambda_{\mathrm{L1}}\lambda_{\mathrm{L2}}}\right) + \Delta I\left(\frac{\lambda_{\mathrm{L2}} - \lambda_{\mathrm{L1}}}{\lambda_{\mathrm{L1}}^2}\right) + (\Delta N_{\mathrm{L1}} - \Delta N_{\mathrm{L2}}) + \left(\frac{\varepsilon_{\Delta\phi,\mathrm{L1}}}{\lambda_{\mathrm{L1}}} - \frac{\varepsilon_{\Delta\phi,\mathrm{L2}}}{\lambda_{\mathrm{L1}}}\right) \tag{25}$$

and

$$\left(\frac{\lambda_{\mathrm{L2}} - \lambda_{\mathrm{L1}}}{\lambda_{\mathrm{L1}} + \lambda_{\mathrm{L2}}}\right)\left(\frac{\Delta PR_{\mathrm{L1}}}{\lambda_{\mathrm{L1}}} + \frac{\Delta PR_{\mathrm{L2}}}{\lambda_{\mathrm{L2}}}\right) = \Delta\rho\left(\frac{\lambda_{\mathrm{L2}} - \lambda_{\mathrm{L1}}}{\lambda_{\mathrm{L1}}\lambda_{\mathrm{L2}}}\right) + \Delta I\left(\frac{\lambda_{\mathrm{L2}} - \lambda_{\mathrm{L1}}}{\lambda_{\mathrm{L1}}^2}\right) + \left(\frac{\lambda_{\mathrm{L2}} - \lambda_{\mathrm{L1}}}{\lambda_{\mathrm{L1}} + \lambda_{\mathrm{L2}}}\right)\left(\frac{\varepsilon_{\Delta PR,\mathrm{L1}}}{\lambda_{\mathrm{L1}}} + \frac{\varepsilon_{\Delta PR,\mathrm{L2}}}{\lambda_{\mathrm{L2}}}\right). \tag{26}$$

Differencing between the widelane carrier phase (25) and the narrowlane code phase (26) results in

$$(\Delta\phi_{\mathrm{L1}} - \Delta\phi_{\mathrm{L2}}) - \left(\frac{\lambda_{\mathrm{L2}} - \lambda_{\mathrm{L1}}}{\lambda_{\mathrm{L1}} + \lambda_{\mathrm{L2}}}\right)\left(\frac{\Delta PR_{\mathrm{L1}}}{\lambda_{\mathrm{L1}}} + \frac{\Delta PR_{\mathrm{L2}}}{\lambda_{\mathrm{L2}}}\right) = (\Delta N_{\mathrm{L1}} - \Delta N_{\mathrm{L2}}) + \left(\frac{\varepsilon_{\Delta\phi,\mathrm{L1}}}{\lambda_{\mathrm{L1}}} - \frac{\varepsilon_{\Delta\phi,\mathrm{L2}}}{\lambda_{\mathrm{L2}}}\right) - \left(\frac{\lambda_{\mathrm{L2}} - \lambda_{\mathrm{L1}}}{\lambda_{\mathrm{L1}} + \lambda_{\mathrm{L2}}}\right)\left(\frac{\varepsilon_{\Delta PR,\mathrm{L1}}}{\lambda_{\mathrm{L1}}} + \frac{\varepsilon_{\Delta PR,\mathrm{L2}}}{\lambda_{\mathrm{L2}}}\right). \tag{27}$$

Equation (27) can be rewritten in the compact form

$$Z_{\Delta w} = N_{\Delta w} + \nu_{\Delta w} \tag{28}$$

where

$$Z_{\Delta w} = (\Delta\phi_{\mathrm{L1}} - \Delta\phi_{\mathrm{L2}}) - \left(\frac{\lambda_{\mathrm{L2}} - \lambda_{\mathrm{L1}}}{\lambda_{\mathrm{L1}} + \lambda_{\mathrm{L2}}}\right)\left(\frac{\Delta PR_{\mathrm{L1}}}{\lambda_{\mathrm{L1}}} + \frac{\Delta PR_{\mathrm{L2}}}{\lambda_{\mathrm{L2}}}\right)$$

$$N_{\Delta w} = (\Delta N_{\mathrm{L1}} - \Delta N_{\mathrm{L2}})$$

$$\nu_{\Delta w} = \left(\frac{\varepsilon_{\Delta\phi,\mathrm{L1}}}{\lambda_{\mathrm{L1}}} + \frac{\varepsilon_{\Delta\phi,\mathrm{L2}}}{\lambda_{\mathrm{L2}}}\right) - \left(\frac{\lambda_{\mathrm{L2}} - \lambda_{\mathrm{L1}}}{\lambda_{\mathrm{L1}} + \lambda_{\mathrm{L2}}}\right) \times \left(\frac{\varepsilon_{\Delta PR,\mathrm{L1}}}{\lambda_{\mathrm{L1}}} + \frac{\varepsilon_{\Delta PR,\mathrm{L2}}}{\lambda_{\mathrm{L2}}}\right).$$

Assuming that $\sigma^{ij}_{\Delta\phi,\mathrm{L1}} = \sigma^{ij}_{\Delta\phi,\mathrm{L2}} \equiv \sigma_{\Delta\phi}$ and $\sigma^{ij}_{\Delta PR,\mathrm{L1}} = \sigma^{ij}_{\Delta PR,\mathrm{L2}} \equiv \sigma_{\Delta PR}$, the variance of the differenced widelane cycle ambiguity estimate error can be written as

$$\sigma^2_{\Delta w} = \left(\frac{1}{\lambda^2_{\mathrm{L1}}} + \frac{1}{\lambda^2_{\mathrm{L2}}}\right)\left(\sigma^2_{\Delta\phi} + \left(\frac{\lambda_{\mathrm{L2}} - \lambda_{\mathrm{L1}}}{\lambda_{\mathrm{L1}} + \lambda_{\mathrm{L2}}}\right)^2 \sigma^2_{\Delta PR}\right). \tag{29}$$

APPENDIX B. VARIANCE OF WIDELANE CYCLE AMBIGUITY ESTIMATE ERROR

Consider a noisy observation of the widelane cycle ambiguity estimate given by (28). A running average of such observables over a time interval T will produce a cycle ambiguity estimate whose error variance can be expressed as [10]

$$\mathrm{var} = \frac{1}{T}\int_0^T \left[1 - \frac{|\tau|}{T}\right] R(\tau)\,d\tau \tag{30}$$

where $R(\tau)$ is the autocorrelation function of the zero-mean, time correlated error $\nu_{\Delta w}$.

In this work, the ranging measurement error is modeled as a first-order Gauss-Markov random process, which has the autocorrelation function

$$R(\tau) = \sigma_{\Delta w} e^{-\beta|\tau|} \tag{31}$$

where $\sigma_{\Delta w}$ is defined in (29) and $1/\beta$ is the correlation time of $\nu_{\Delta w}$. Substituting (31) into (30) yields

$$\mathrm{var} = \frac{2\sigma^2}{T\beta} - \frac{2\sigma^2}{T^2\beta^2}(1 - e^{-T\beta}). \tag{32}$$

REFERENCES

[1] JPALS Test Planning Working Group
Architecture and Requirements Definition: Test and Evaluation Master Plans for JPALS, Jan. 19, 1999.

[2] Operational Requirements Document (ORD) for Joint Precision Approach and Landing System (JPALS), USAF 002-94-I.

[3] Pervan, B., Chan, F., Gebre, D., Pullen, S., Enge, P., and Colby, G.
Performance analysis of carrier phase DGPS navigation for shipboard landing of aircraft.
Navigation, **50**, 3 (Fall 2003).

[4] Euler, H-J., and Goad, C.
On optimal filtering of GPS dual frequency observations without using orbit information.
Bulletin Geodesique, Vol. 61, New York: Springer-Verlag, 1991.

[5] Hwang, P., McGraw, G., and Bader, J.
Enhanced differential GPS carrier-smoothed code processing using dual-frequency measurements.
Navigation, **46**, 2 (1999).

[6] Gao, Y., and Li, Z.
Cycle slip detection and ambiguity resolution algorithms for dual-frequency GPS data.
Marine Geodesy, **22**, 4 (1999).

[7] *Global Positioning System Standard Positioning Service Performance Standard*, Oct. 2001, www.navcen.uscg.gov/pubs/gps/sigspec.

[8] Misra, P., and Enge, P.
Global Positioning System: Signals, Measurements, and Performance, Lincoln, MA: Ganga-Jamuna Press, 2001.

[9] Teunissen, P., Odijk, D., and Joosten, P.
A probabilistic evaluation of correct GPS ambiguity resolution.
In *Proceedings of the Tenth International Technical Meeting of the Satellite Division of the Institute of Navigation*, Nashville, TN, Sept. 15–18, 1998.

[10] Bendat, J. S., and Piersol, A. G.
Random Data: Analysis and Measurement Procedures (3rd ed.).
New York: Wiley, 2000.

[11] Shively, C.
Satellite criticality concepts for unavailability and unreliability of GNSS satellite navigation.
Navigation, **40**, 4 (Winter 1993–94).

Moon-Beom Heo received a B.S. in mechanical engineering from Kyung-Hee University, Korea, in 1992, and the M.S. and Ph.D. degrees in mechanical and aerospace engineering from the Illinois Institute of Technology, Chicago, respectively, in 1997 and 2004.

He is currently a senior researcher in the Space Application Center/Space Science Group of the Korea Aerospace Research Institute (KARI) in Daejeon, Korea. His work is focused on Global Navigation Satellite Systems (GNSS) and their augmentation.

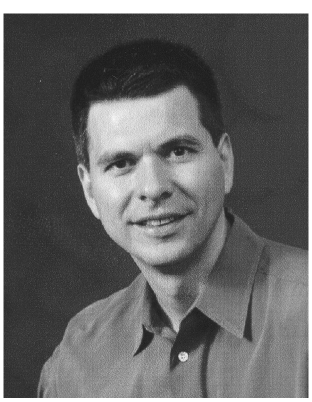

Boris Pervan received the B.S. from the University of Notre Dame, Notre Dame, IN, the M.S. from California Institute of Technology, Pasadena, and the Ph.D. from Stanford University, Stanford, CA.

He was a spacecraft mission analyst at Hughes Space and Communications Group (now Boeing) and was project leader at Stanford University for GPS LAAS research and development. He is currently an associate professor of mechanical and aerospace engineering at the Illinois Institute of Technology, Chicago.

Dr. Pervan was the recipient of the Sigma Xi Excellence in University Research Award (2005), University Excellence in Teaching Award (2005), Ralph Barnett Mechanical and Aerospace Engineering Department Outstanding Teaching Award (2002), IEEE Aerospace and Electronics Systems Society M. Barry Carlton Award (1999), RTCA William E. Jackson Award (1996), Guggenheim Fellowship (Caltech 1987), and Albert J. Zahm Prize in Aeronautics (Notre Dame 1986). He is currently an associate editor of the journal *Navigation*.